MR Imaging–guided Breast Localization System with Medial or Lateral Access[1]

Petrina A. Causer, MD
Cameron A. Piron, MSc
Roberta A. Jong, MD
Belinda N. Curpen, MD
Chris A. Luginbuhl, BEng
Joan E. Glazier, MRT (R) CBI
Ellen Warner, MD
Kimberley Hill, BA
Joanne Muldoon, MRT (R) (MR)
Glen Taylor, MD
John W. Wong, MD
Donald B. Plewes, PhD

Purpose: To evaluate the degree of error of the authors' magnetic resonance (MR) imaging–guided needle localization system for biopsy of suspicious lesions visualized only with MR imaging, by using both prospectively recorded and retrospectively reviewed data, including MR imaging lesion coordinates as the reference standard, and to determine whether any lesion or breast characteristics affect this error.

Materials and Methods: Institutional review board approval, along with informed consent, was obtained as directed by the board. In 31 patients (age range, 34–64 years; mean age, 54.5 years), 38 wires were placed for 35 lesions by means of an MR-guided needle localization system with medial or lateral access and computer software assistance for needle placement calculation. Needle and wire placement error measurements were calculated before and after necessary placement correction, accounting for tissue shift in the z plane. The error was statistically correlated with MR imaging lesion variables, breast density, and histopathologic findings by means of univariate and multivariate linear regression analyses or two-tailed paired *t* test. Procedure times and the frequency of medial or lateral approaches were recorded.

Results: Eleven of 35 localizations (31%) were medial, and 24 of 35 (69%) were lateral. The mean total magnet time was 61.6 minutes, and the mean needle deployment time was 9 minutes (range, 4–17 minutes). Sixteen of 35 lesions (46%) were malignant (seven ductal carcinoma in situ, six invasive ductal, two invasive lobular, and one lymphoma). The mean uncorrected needle placement error was 1.3 mm (range, 0–6 mm) for the x plane, 2.4 mm (range, 0–6.5 mm) for the y plane, and 5.6 mm (range, 0–15.6 mm) for the z plane. Fourteen of 38 needles (37%) required repositioning for z-plane error. The corrected z-plane error improved to 3.2 mm (range, 0–10.0 mm). Factors that significantly increased the uncorrected error included tissue shift in the z plane ($R = 0.7$), small lesion size ($R = -0.59$), and fatty breast density ($P = .029$).

Conclusion: The authors' system is accurate for performing MR-guided needle localizations for both medial and lateral approaches. Factors that increased the uncorrected needle placement error included small lesion size, fatty breast density, and tissue shift in the z plane.

[1] From the Departments of Medical Imaging (P.A.C., R.A.J., B.N.C., J.E.G.), Imaging Research (C.A.P., C.A.L., J.M., D.B.P.), Medical Biophysics (C.A.P., C.A.L., J.M., D.B.P.), Surgical Oncology (G.T.), and Anatomic Pathology (J.W.W.); and Division of Medical Oncology, Department of Medicine (E.W., K.H.), Sunnybrook Health Sciences Centre, 2075 Bayview Ave, MG166, Toronto, ON, Canada M4N 3M5. From the 2003 RSNA Annual Meeting. Received August 5, 2004; revision requested October 12; revision received March 21, 2005; accepted April 21; final version accepted September 1. Supported by the Canadian Breast Cancer Research Initiative, Terry Fox Foundation of the National Cancer Institute of Canada, the Ontario Research and Development Challenge Fund, and Amersham Health. **Address correspondence to** P.A.C. (e-mail: *Petrina.causer@sw.ca*).

There are many clinical applications of breast magnetic (MR) resonance imaging in the evaluation of breast cancer, including preoperative assessment of the extent of disease, screening of the contralateral breast in women with known cancer, a problem-solving complement to conventional imaging with mammography and ultrasonography (US), and screening of high-risk women (1). A standard approach to work-up of a Breast Imaging Reporting and Data System (BI-RADS) category 4–5 lesion detected with MR imaging is to review the standard mammograms again, possibly obtain additional mammographic views, and perform targeted second-look US in an attempt to identify the lesion. If the lesion is visualized with another modality, this would allow a standard means of biopsy guidance (2). However, cancers that are truly visible only at MR imaging are detected in 14%–35% of patients examined with breast MR imaging for a variety of indications (2,3). The reported sensitivities of MR imaging for detecting malignancy are high. For invasive carcinoma, sensitivities range from 81% to 100% for screening and diagnostic settings. For ductal carcinoma in situ, they are more variable, ranging from 40% to 100% (4–12). For invasive carcinoma, the sensitivity of MR imaging is higher than that reported for mammography and US, making it a desirable addition to available conventional imaging. As with mammography and US, however, the reported specificities are variable, ranging from 30% to 83% (13–19), necessitating a means of tissue sampling and pathologic assessment.

Cancers detected only with MR imaging can be small lesions to target for biopsy, with reported sizes of invasive cancers detected at screening MR imaging as small as 0.1 cm (1). It can be challenging to perform accurate biopsies of these lesions. There are well-established means to perform percutaneous biopsy or localization and surgical biopsy with conventional mammographic or US guidance. The reported experience with MR-guided techniques is limited but increasing (3,20–33). Several issues are unique to MR-guided needle localizations and biopsies, including limited access to the entire breast (most available systems provide lateral access to the breast and reduced access near the chest wall), limits on procedure time due to limited MR imaging resources, and the brief interval before washout of lesion enhancement or obscuring by background parenchymal enhancement for many lesions.

While the accuracy of needle and wire placement is important with any means of guidance, it is particularly important for MR-guided procedures. This is because lesion retrieval cannot be verified with radiography of the lumpectomy specimen, as the lesion is most often visible only in vivo after intravenous administration of gadolinium-based contrast material.

The purpose of our study was to evaluate the degree of error of our MR-guided needle localization system for biopsy of suspicious lesions visualized only with MR imaging, by using both prospectively recorded and retrospectively reviewed data, including lesion MR imaging coordinates as the reference standard, and to determine whether any lesion or breast characteristics affect this error.

Materials and Methods

Patients

Our institutional review board approved both the retrospective review of the patient's images and records and the prospective collection of data at the time of MR-guided localization. Patient informed consent was obtained for use of the localization system, but the institutional review board did not require patient consent for the retrospective review of data. MR-guided needle localizations were recommended for 37 lesions in 33 patients and were performed for 35 lesions in 31 patients, who formed the final patient group. The mean patient age was 54.5 years (range, 34–64 years).

One patient required repeated localization on a second date for the same lesion that was missed at the initial surgery, therefore requiring two wires placed for the same lesion. Two of the original 33 patients (6.1%) for whom localization was recommended had a nonenhancing lesion on the date of the procedure. These localizations were therefore cancelled, decreasing the final patient population to 31. Two of the 35 lesions included in our study were bracketed with two wires, for a total of 38 wires placed.

The majority of patients (28 of 31 patients [90%]) underwent initial MR imaging for screening as high-risk patients. These included 18 patients participating in an ongoing study evaluating MR imaging for screening due to a known *BRCA1* or *BRCA2* genetic mutation or as a first-degree relative of a known mutation carrier (4,34), five patients with a personal history of breast cancer, four patients with a very strong family history of breast or ovarian cancer, and one patient with a high-risk marker at prior biopsy and an associated family history. Of the remaining three patients (9.7%), two were examined with MR imaging as a problem-solving complement to conventional imaging with mammography and US and one was examined to determine the preoperative extent of disease. In all three patients, MR imaging depicted an additional lesion that had been occult at conventional imaging (atypical ductal hyperplasia in two patients, lymphoma in one patient).

Published online before print
10.1148/radiol.2401041368

Radiology 2006; 240:369–379

Abbreviations:
BI-RADS = Breast Imaging Reporting and Data System
SPGR = spoiled gradient recalled

Author contributions:
Guarantor of integrity of entire study, P.A.C.; study concepts/study design or data acquisition or data analysis/interpretation, all authors; manuscript drafting or manuscript revision for important intellectual content, all authors; manuscript final version approval, all authors; literature research, P.A.C.; clinical studies, P.A.C., C.A.P., R.A.J., B.N.C., E.W.; statistical analysis, C.A.P., D.B.P.; and manuscript editing, all authors

Authors stated no financial relationship to disclose.

Diagnostic Breast MR Imaging Technique and Interpretation

Bilateral breast MR imaging was performed in the sagittal plane, according to one of two techniques, with a 1.5-T system (Signa; GE Medical Systems, Milwaukee, Wis). The most frequently used protocol (used for 22 of 31 patients [71%]) was performed on our research MR system with specialized breast coils and bilateral imaging pulse sequences that were available only on our research magnet. The second protocol was performed on our clinical system with commercially available breast surface coils (MRI Devices, Waukesha, Wis) and pulse sequences. The coils and pulse sequences used on the research system have been previously described (4,34,35); they include a phased-array bilateral breast coil and a slab-interleaved bilateral pulse sequence, similar to that described by Greenman et al (36). Follow-up MR imaging at high temporal and spatial resolution was later performed for all BI-RADS category 0 and 3–5 lesions (37). This protocol has also been previously described (4,34).

The second bilateral sequential sagittal MR imaging protocol used (nine of 31 patients [29%]) included a multiplanar localizing sequence—T1-weighted two-dimensional fast spoiled gradient-recalled (SPGR)—followed by sagittal fat-suppressed T2-weighted fast spin-echo (4000–6000/85 [repetition time msec/echo time msec]) and T1-weighted three-dimensional SPGR with spectral inversion at lipid, or SPECIAL (8.8/4.2; flip angle, 10°), sequences performed before and three times after a rapid bolus intravenous injection of 0.1 mmol/L of gadodiamide (Omniscan; Amersham Health, Oakville, Ontario, Canada). Each volumetric acquisition was performed in less than 2 minutes. Section thickness was 2–3 mm, without a gap and with a 256 × 192 matrix and a 16–20-cm field of view. Precontrast images were subtracted from postcontrast images.

MR images were interpreted on a picture archiving and communication system (Impax; AGFA, Toronto, Ontario, Canada) by one of three breast imaging specialists (P.A.C., R.A.J., B.N.C.), who had 3, 2.5, and 1 year of breast MR imaging experience, respectively. Interpretation included use of established BI-RADS criteria, which were based on lesion morphologic and enhancement characteristics (37). Our study included only those patients who had an MR imaging–detected BI-RADS 4 or 5 lesion with no mammographic or sonographic correlate. This conventional imaging included targeted, second-look US with possible additional mammographic work-up.

MR Imaging–guided Needle Localization Procedure

The localizations were performed by one of two radiologists (P.A.C., R.A.J.) with a system designed at our institution, which features a fundamental redesign of the MR imaging bed and coil system that allows both lateral and medial approaches (Fig 1). MR-guided needle positioning was accomplished with a device that supports two fenestrated plates (6 × 8 array of rectangular 5/8-inch apertures) that provided mediolateral compression of the breast. Fine needle positioning within these fenestrations was performed by using guide plugs. An array of drilled guide holes in these plugs provided a means of delivering a needle into the breast through a finite number of positions (2.5-mm centers for 20-gauge needles) (Fig 1). A pair of MR-visible fiducial markers was positioned at known locations relative to the fenestrations. Imaging was achieved with a pair of phased-array MR coils attached to the compression plates. The location of the lesion was determined from the MR imaging coordinates of the enhancing lesion relative to the fiducial markers. A computer program was used to help locate the

Figure 1

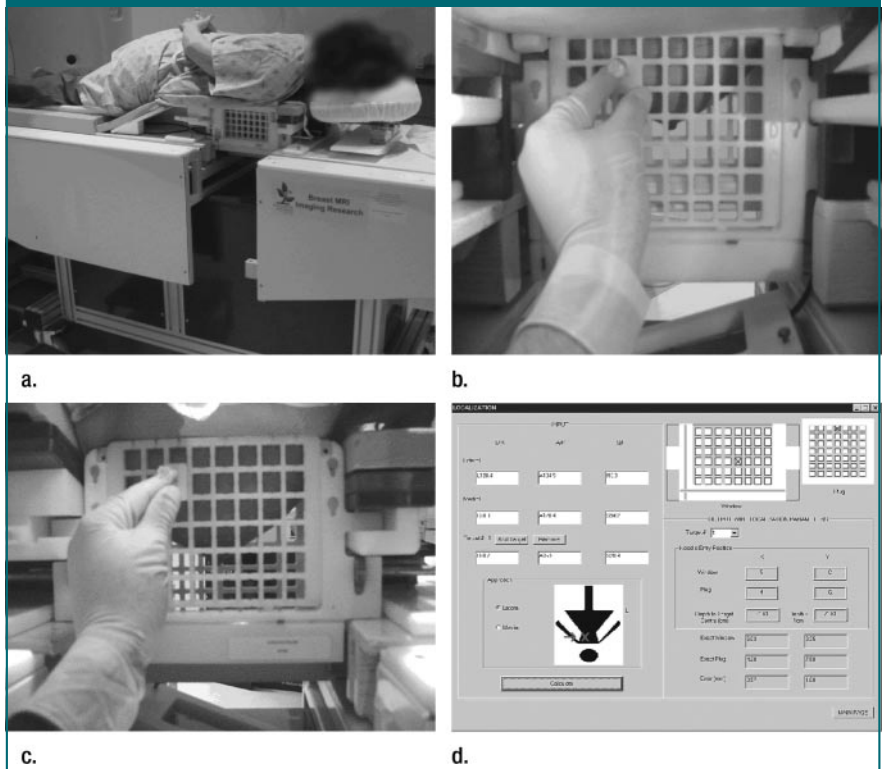

Figure 1: Breast MR imaging localization device. **(a)** Patient positioned prone on the MR imaging bed with coil and medial or lateral access grid localization device for lateral approach localization. **(b)** Medial and **(c)** lateral access views of the grid and needle guides with needle placement. **(d)** Computer software interface for calculation of needle trajectory from a medial or lateral approach.

appropriate fenestration, guide hole, and needle insertion depth to intercept the lesion of interest on the basis of the location of the fiducial markers and the lesion location on the MR images (Fig 1).

For each procedure, the breast was cleansed with chlorhexidine 0.5% (Laboratoire Atlas, Montreal, Quebec, Canada). The patient was positioned prone, and her breast was placed within the sterile grid localizing device; a sterile technique was used.

MR imaging was then performed. Localizer images were initially obtained in all patients to determine the coordinates of the fiducial markers. Only data from the phase-encoding direction were used, to overcome spatial distortion due to perturbations to the main magnetic field of the imaging system caused by magnetic susceptibility variations arising from the presence of the patient and apparatus in the imaging volume. Imaging included transverse localizer and coronal sequences and an additional coronal localizer sequence with the frequency and phase directions swapped.

Sagittal images were then obtained, with the choice of protocol dependent on how the lesion was best visualized at the diagnostic MR study. If a lesion was best seen with high-spatial-resolution imaging, three-dimensional SPGR T1-weighted fat-suppressed imaging was performed before and after gadolinium enhancement (imaging parameters provided above) until the enhancing lesion was visualized. If a lesion was best seen with a high-temporal-resolution protocol, two-dimensional SPGR T1-weighted fat-suppressed imaging was performed before and after administration of contrast material (parameters described earlier), again until the lesion was visualized (Fig 2).

A set of transverse fat-suppressed two-dimensional SPGR T1-weighted images (150/4.2; flip angle, 50°) was obtained through the region of the lesion (Fig 2). Each acquisition was obtained in 20 seconds. The section thickness was 2.5 mm, without a gap and with a 256 × 128 matrix and an 18-cm field of view. The coordinates of the lesion were determined by placing a cursor over the lesion at the MR monitor, and the values were entered into the computer program. The computer program calculated the needle trajectory, including the grid coordinate, needle guide fenestration, and needle insertion depth. The computer program calculated the targeted depth 1 cm beyond the lesion to allow final wire position at that depth.

The patient was withdrawn from the magnet, and the skin was again cleansed with chlorhexidine 0.5%. The needle guide was inserted into the appropriate grid hole, and the skin and subcutaneous tissue were locally anesthetized with 1–2 mL of 1% lidocaine hydrochloride (Abbott Laboratories, Chicago, Ill). The MR-compatible needle and hookwire (20-gauge MRI Compatible Lesion Marking System with Wire, EZ-EM, Westbury, NY; MReye Modified Disp Spring Hook Localization Needle, Cook, Bloomington, Ind) were inserted into the calculated grid hole and fenestration of the needle guide to the appropriate depth.

The patient was placed back in the magnet, and both sagittal and transverse images were obtained with the needle in place (Fig 2). To confirm accurate needle placement, the position of the needle with respect to the lesion was visually assessed, and the needle tip placement was compared with the initial lesion coordinates. For most patients, any variation of 5 mm or more required repositioning of the needle, depending on the size of the lesion targeted. Due to needle artifact as large as 8 mm in diameter in the sagittal plane, small lesions of about this size were often obscured. The blooming artifact of the needle and wire tip was also compensated for to establish their true positions in the breast.

Alternatively, some lesions that enhanced and then had rapid enhancement washout were not directly visualized. In such cases, the initial lesion coordinates and surrounding anatomic tissue interface landmarks were compared to identify tissue shift after needle insertion. After the patient was removed from the magnet, any necessary needle adjustments were made to account for these factors, and the wire was deployed. A final set of transverse images was obtained through the region of the lesion and wire. For the last five of 31 patients (16%), a final set of transverse images was obtained after release of the mild mediolateral compression, because of the recognized "accordion effect" (28,38) and subsequent risk of the wire backing out.

After localization, the wire was secured to the skin with tape, and two-view mammograms were obtained. The mammograms were labeled to serve as a road map for the surgeon, and they, along with a written procedure note, were taken to the operating room with the patient.

Data and Statistical Analyses

One imaging researcher (C.A.P.) prospectively collected a record of data, including use of medial versus lateral approach, the fiducial and lesion MR imaging coordinates, the presence and value of tissue shift measurements after needle placement, the visibility of the lesion with the needle and wire in place, and wire placement coordinates for each localization. The procedure time, including the total magnet time required for each procedure and each step of the procedure, was prospectively recorded as follows: MR imaging table setup, patient preparation, MR imaging, needle and wire placement, and patient removal from the magnet room.

The MR images for each initial diagnostic MR imaging study and localization procedure were retrospectively reviewed by one breast radiologist (P.A.C.). Lesion characteristics, including morphologic type (mass vs nonmass lesion), and enhancement characteristics, including degree of initial enhancement and delayed pattern of enhancement, were evaluated according to established BI-RADS criteria (37). Lesion size and depth in the breast from the closest medial or lateral skin surface were also determined. Preoperative and post–needle localization mammograms were also retrospectively assessed for breast density, both overall and localized to the area surrounding the lesion, and categorized according to

BI-RADS criteria by the same breast radiologist (37). Lesion pathologic findings were determined from surgical pathology reports and were categorized as benign, malignant, or a high-risk marker. All patients, except those who underwent bilateral mastectomy after localization (six of 31 patients [19%]), underwent follow-up MR imaging to ensure the lesion was excised. MR imaging lesion characteristics and breast density were evaluated according to histopathologic findings, and the number of missed lesions was determined.

Needle and wire placement error

Figure 2

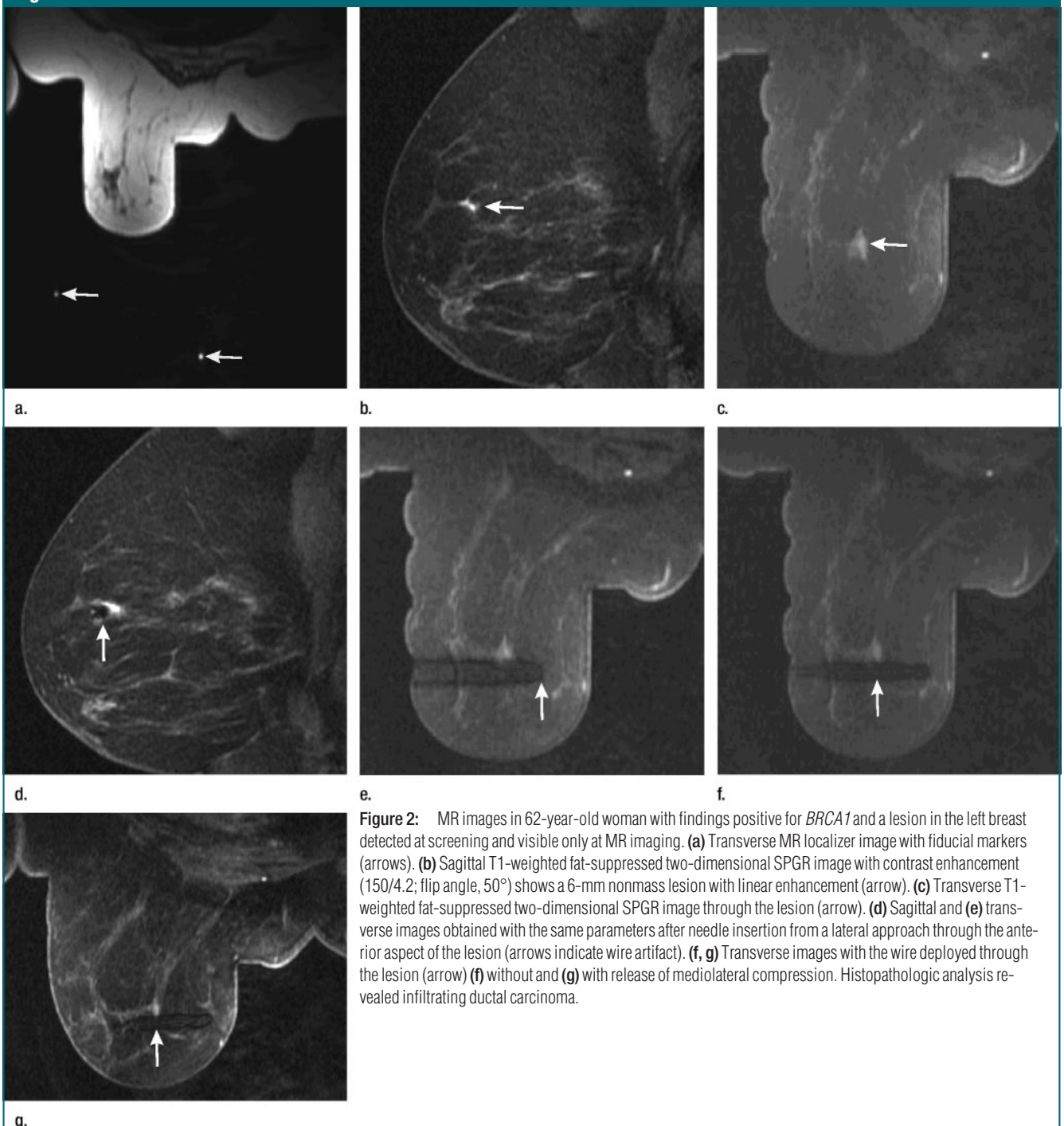

Figure 2: MR images in 62-year-old woman with findings positive for *BRCA1* and a lesion in the left breast detected at screening and visible only at MR imaging. **(a)** Transverse MR localizer image with fiducial markers (arrows). **(b)** Sagittal T1-weighted fat-suppressed two-dimensional SPGR image with contrast enhancement (150/4.2; flip angle, 50°) shows a 6-mm nonmass lesion with linear enhancement (arrow). **(c)** Transverse T1-weighted fat-suppressed two-dimensional SPGR image through the lesion (arrow). **(d)** Sagittal and **(e)** transverse images obtained with the same parameters after needle insertion from a lateral approach through the anterior aspect of the lesion (arrows indicate wire artifact). **(f, g)** Transverse images with the wire deployed through the lesion (arrow) **(f)** without and **(g)** with release of mediolateral compression. Histopathologic analysis revealed infiltrating ductal carcinoma.

measurements for both the x (superoinferior) and y (anteroposterior) planes were calculated from the sagittal MR images by determining the difference in the needle and wire placements and the initially targeted lesion position coordinates. The reference standard was the lesion MR coordinates after needle and wire placement, if the lesion was visualized with the needle or wire in place, or the original lesion coordinates from the localizing enhanced MR images, if the lesion was not visible with the needle and wire in place.

The error measurement for the transverse or z plane (through plane) was similarly calculated. The reference standard was either the lesion MR coordinates, used when the lesion was visible with the needle and wire in place, or the initial lesion coordinates, used when the lesion was not visualized after needle and wire placement. A tissue shift measurement was added for the latter group when a tissue shift was present. Once the appropriate MR coordinates for each procedure were determined, 10 mm was added to account for the final desired placement of the wire beyond the lesion, and those MR coordinates were compared with the tip of the needle or wire artifact. The measurement of either the needle artifact or the wire artifact was also taken into account for the needle and wire coordinate values. The number of repositioned needles and the error measurements of these needle placement corrections were also determined. The uncorrected needle and final wire placement error measurements were compared with the corrected values.

All statistical calculations, including those made by using univariate and multivariate linear regression analyses and the Student *t* test, were performed with software (Excel 2002; Microsoft, Redmond, Wash). Both the uncorrected and the corrected needle and wire placement error measurements were individually correlated with the MR imaging lesion variables of lesion size and lesion depth and with the tissue shift measurement. Linear regression analysis was used to determine the strength of the relationship between accuracy and these continuous variables. The strength of this relationship was defined by using R values and analyzed with both univariate and multivariate linear regression analyses.

To address the possibility that motion in the sagittal x or y plane was associated with motion in the transverse z plane, the z-error measurement was decorrelated from the x or y plane error by means of linear detrending performed with Excel. A two-tailed paired *t* test was used to correlate error measurements with lesion variables, including morphologic type (mass vs nonmass), enhancement characteristics, medial versus lateral approach, breast density at mammography, and pathologic diagnosis (malignant vs benign). The variables were sorted according to each of these criteria and then compared with determine whether they were statistically significant. In all statistical calculations, P values less than .05 were considered to denote statistical significance.

Table 1

MR Imaging Lesion and Breast Density Characteristics according to Histopathologic Findings

Characteristic	Total ($n = 35$)	Malignant ($n = 16$)	Benign ($n = 16$)	High-Risk Marker ($n = 3$)
Morphologic type				
Mass	20 (57)	10 (63)	8 (50)	2 (67)
Nonmass	15 (43)	6 (38)	8 (50)	1 (33)
Early enhancement				
Mild	5 (14)	0 (0)	5 (31)	0 (0)
Moderate	16 (46)	10 (63)	4 (25)	2 (67)
Marked	14 (40)	6 (38)	7 (44)	1 (33)
Delayed enhancement				
Persistent	11 (31)	4 (25)	6 (38)	1 (33)
Plateau	12 (34)	5 (31)	6 (38)	1 (33)
Washout	12 (34)	7 (45)	4 (25)	1 (33)
Overall density				
Fatty	9 (26)	3 (19)	5 (31)	1 (33)
Scattered fibroglandular	8 (23)	6 (38)	2 (13)	0 (0)
Heterogeneously dense	11 (31)	4 (25)	6 (38)	1 (33)
Dense	7 (20)	3 (19)	3 (19)	1 (33)
Localized density				
Fatty	8 (23)	3 (19)	4 (25)	1 (33)
Scattered fibroglandular	8 (23)	5 (31)	4 (25)	0 (0)
Heterogeneously dense	14 (40)	6 (38)	5 (31)	2 (67)
Dense	5 (14)	2 (13)	3 (19)	0 (0)

Note.—Data are numbers of lesions. Numbers in parentheses are percentages.

Results

Procedures

Localizations were performed between July 1999 and December 2003. The mean total magnet time, from the preprocedure setup to the time the patient exited the MR suite, was 62 minutes (range, 45–80 minutes). The mean localization time, from the moment the lesion was visualized at the console to the moment when the final wire placement was confirmed, was 9.0 minutes (range, 4–17 minutes). For five patients, two wires were placed, with a mean time of 11.7 minutes (range, 8–17 minutes) for both wires. This compares with a mean of 7.5 minutes (range, 4–15 minutes) to place a single wire in the remaining 28 patients. Eleven of 35 lesions (31%) were localized from a medial approach, and 24 (69%) were localized from a lateral approach. There were no complications related to the procedure.

Lesion Characteristics

The mean lesion size was 12.4 mm (range, 4–35 mm), and the mean lesion

depth within the breast was 22.6 mm (range, 6–48 mm). Pathologic analysis of the 35 localized lesions revealed 16 malignant lesions (46%) (seven ductal carcinomas in situ, six invasive ductal carcinomas, two invasive lobular carcinomas, and one lymphoma) and three high-risk markers (8.6%) (atypical ductal hyperplasia). Twenty of 35 lesions (57%) had a mass morphology, and the remaining 15 (43%) were nonmass lesions. Most lesions had either moderate (16 of 35 lesions [46%]) or marked (14 of 35 lesions [40%]) early enhancement. The delayed enhancement pattern was relatively equally distributed, with a persistent pattern in 11 of 35 lesions (31%), a plateau in 12 lesions (34%), and washout in 12 lesions (34%). The overall breast density was fatty in nine of 35 lesions (26%), scattered fibroglandular in eight lesions (23%), heterogeneously dense in 11 lesions (31%), and dense in seven lesions (20%). The localized breast density was fatty in eight of 35 lesions (23%), scattered fibroglandular in eight lesions (23%), heterogeneously dense in 14 lesions (40%), and dense in five lesions (14%). The numbers were too small for us to perform subset analysis to determine any significant differences in MR imaging lesion and breast density characteristics according to histopathologic findings (Table 1).

The mean tissue shift measured in the z, or through, plane after needle placement was 3.8 mm (range, 0–9 mm). A tissue shift of 4 mm or more was considered important and occurred with 24 of 38 needles placed (63%). Needles required repositioning if their position was at least 5 mm from the target. This occurred for 14 of the 38 needles placed (37%) owing to initial inaccurate placement and/or tissue shift. Once the needle was placed, 10 of 35 lesions (29%) were not visualized. Seven lesions 8 mm or smaller were obscured by needle artifact, and in the other three lesions, washout had occurred by the time the needle was placed. Needle localization was recommended but not performed in two of 33 patients (6%) because the lesion did not enhance at the time of the procedure.

Table 2

Error Measurements for All 38 Needles Placed

	Mean Error (mm)		
Error Correction	x-Axis (Superoinferior)	y-Axis (Anteroposterior)	z-Axis (Left-Right)
Uncorrected	1.3 (0–6)	2.4 (0–6.5)	5.6 (0–15.6)
Corrected	NA	NA	3.2 (0–10.0)

Note.—Numbers in parentheses are ranges. NA = not applicable.

Table 3

Error Measurements for 14 Repositioned Needles

	Mean Error (mm)		
Error Correction	x-Axis (Superoinferior)	y-Axis (Anteroposterior)	z-Axis (Left-Right)
Uncorrected	1.1 (0–2.5)	1.9 (0–3.5)	8.5 (1.0–15.6)
Corrected	NA	NA	3.4 (1.0–8.0)

Note.—Numbers in parentheses are ranges. NA = not applicable.

Both of these patients have since undergone 6-month follow-up MR imaging. At follow-up, the lesions again did not enhance, and they are therefore considered benign.

The mean three-plane error measurements for the 38 needles placed were greatest in the z plane: 5.6 mm (range, 0–15.6 mm) for the uncorrected measurements and 3.2 mm (range, 0–0.0 mm) for the corrected measurements (Table 2). Repositioning was not necessary for in-plane (x- or y-plane) error. There was no significant change in degree of error once the z-plane error was decorrelated from the x- or y-plane error.

The 14 needles that required repositioning also had the greatest error measurements in the z plane. The uncorrected z-plane error measurements ranged from 4.2 to 8.6 mm, and the corrected measurements ranged from 4.0 to 9.9 mm (Table 3). According to linear regression analysis, both tissue shift ($R = 0.7$, $P < .02$) and lesion size ($R = -0.59$, $P < .05$) were moderately correlated with the uncorrected error. Multivariate analysis was performed, and the results validated these correlations, as both tissue shift and lesion size yielded significant relations ($P < .05$ and $P < .05$, respectively). A correlation no longer existed once needle placement was corrected at both univariate and multivariate analyses. Lesion depth within the breast was not significantly correlated with error in any studies (Table 4).

The greatest degree of error based on mammographic breast density occurred for fatty breasts, with error measurements of 8.6 and 9.9 mm, respectively, for overall and localized fatty breast density (Table 5). The differences in error according to overall and localized breast densities were calculated with a two-tailed paired *t* test. For overall breast density, there was a significant difference between fatty and dense breasts. For localized breast density, there were significant differences between fatty and both heterogeneously dense and dense breasts. There were no significant differences in error for the remaining variables, according to two-tailed paired *t* test results.

Three of 35 lesions targeted (8.6%) were missed at surgery. One lesion had an initial pathologic diagnosis of ductal carcinoma in situ, which was thought to be concordant with the MR imaging features. The lesion was found to be persistent at routine follow-up screening approximately 4 months after surgery, which included MR imaging as part of the study protocol. Relocalization and surgical excision revealed ductal carci-

noma in situ again at pathologic analysis, and subsequent follow-up MR imaging demonstrated that the lesion had been successfully removed. The second lesion was found to be a papilloma at pathologic analysis. This patient has been followed up with MR imaging for over 2 years; the lesion has remained stable and is considered benign (Fig 3). The third lesion was diagnosed as stromal fibrosis at pathologic analysis. At postoperative MR imaging, performed owing to discordance between imaging and pathologic findings, the lesion was recognized as remaining within the breast. The patient was reluctant to undergo reexcision and requested close follow-up with MR imaging at 4-month intervals. To date, the lesion has remained stable for 1 year.

Discussion

Needle and wire placement for MR-guided preoperative needle localization can be performed relatively quickly with our system, which includes computer software assistance for needle trajectory calculation. Our mean procedure time was 9 minutes, from lesion visualization to confirmation of final wire placement. Our actual procedure times were faster than the 15–59 minutes previously reported (28,39) for MR-guided localization procedures. However, the mean total magnet time in our study, from table setup to the moment the patient exited the magnet room, was 62 minutes, similar to previously reported times of approximately 1 hour (20,21).

The system used in our study also allows for accurate needle and wire placement, with mean x-, y-, and z-plane errors of 1.3, 2.4, and 5.6 mm, respectively. The final error measurement for needle and wire placement improved in the z plane to 3.2 mm once any necessary needle repositioning was performed; this also accounted for tissue shifts. The sagittal plane error remained constant. Previously reported mean errors have ranged from 1.2 mm to 1 cm and have been provided for one plane, and in most instances, the plane has not been specified (20,28,39). It is therefore difficult to compare directly the degrees of error between our results and those of others. The final wire position, within 5 mm of the targeted lesion, was achieved after the needle was repositioned in 37% of the cases. However, the time for repositioning is negligible and is accounted for in the reported wire placement time. Accurate placement is important for needle localizations to ensure surgical excision of the lesion in question. However, surgical biopsy after needle localization is a relatively forgiving procedure because of the volume of tissue removed around the end of the wire at surgery. Moreover, with the advent of MR-guided vacuum-assisted biopsies, the accuracy of needle placement will become even more important.

Another benefit of our system is the ease of achieving medial access for breast intervention. In our study, we found that a medial approach was required in 31% of our lesions. The limitations associated with the lack of medial access have been described by many authors who were using other systems (20–22,24,28,39). However, our method allows for optimized surgical management, following the principle of traversing the least amount of breast tissue possible to localize a lesion, which is used in mammographically and US-guided localizations.

Factors that significantly affected the degree of error for placement of the needle included lesion size, breast density, and tissue shift in the z, or through, plane. The greatest degree of error occurred for small lesions, in fatty breasts (both overall and in the region surrounding the lesion), and for larger tissue shifts. Once any necessary needle repositioning was performed, with the initial needle placement at least 5 mm from the initial target and tissue shifts in the z plane taken into account, the variables no longer significantly affected the final needle and wire placement errors. One possible explanation for the initial increased error is the increased difference in tissue density between the lesion and surrounding parenchyma, which may cause the lesion to be deflected more readily from the advancing needle.

Small lesion size is important, as lesions 8 mm or smaller are obscured by needle artifact at the time of localization. This problem is confounded by the fact that small lesion size is an important independent variable that increases needle placement error. The radiologist performing the procedure must therefore be vigilant about accurate needle placement for such lesions.

Tissue shift in the z plane is also an important factor affecting error. We believe that the addition of imaging in the plane perpendicular to the initial imaging plane before and after needle insertion helps to avoid placement errors in the through plane. Initial needle placement inaccuracies in the z plane were of greatest importance, as needle readjustments were not necessary for sagittal plane error.

Our rate of missed lesions (8.6%) was higher than that reported by other authors for MR-guided needle localizations (2%–3%) (24,28). However, this rate does fall within the range of 0%–17.9% reported for mammographically guided localizations (40). One potential explanation for our higher recognized miss rate is our 100% follow-up rate with postoperative MR imaging, compared with the previously reported fol-

Table 4

Correlations between Error and Lesion Variables

Variable	Uncorrected *R* Value	Corrected *R* Value
Tissue shift	0.7	0.007
Lesion size	−0.59	−0.17
Depth in breast	−0.18	0.016

Table 5

Mean Errors Based on Overall and Localized Breast Density

	Mean Error (mm)	
Density Type	Overall Density	Localized Density
Fatty	8.6	9.9
Scattered fibroglandular	6.0	4.0
Heterogeneously dense	5.1	4.4
Dense	4.2	5.2

Figure 3

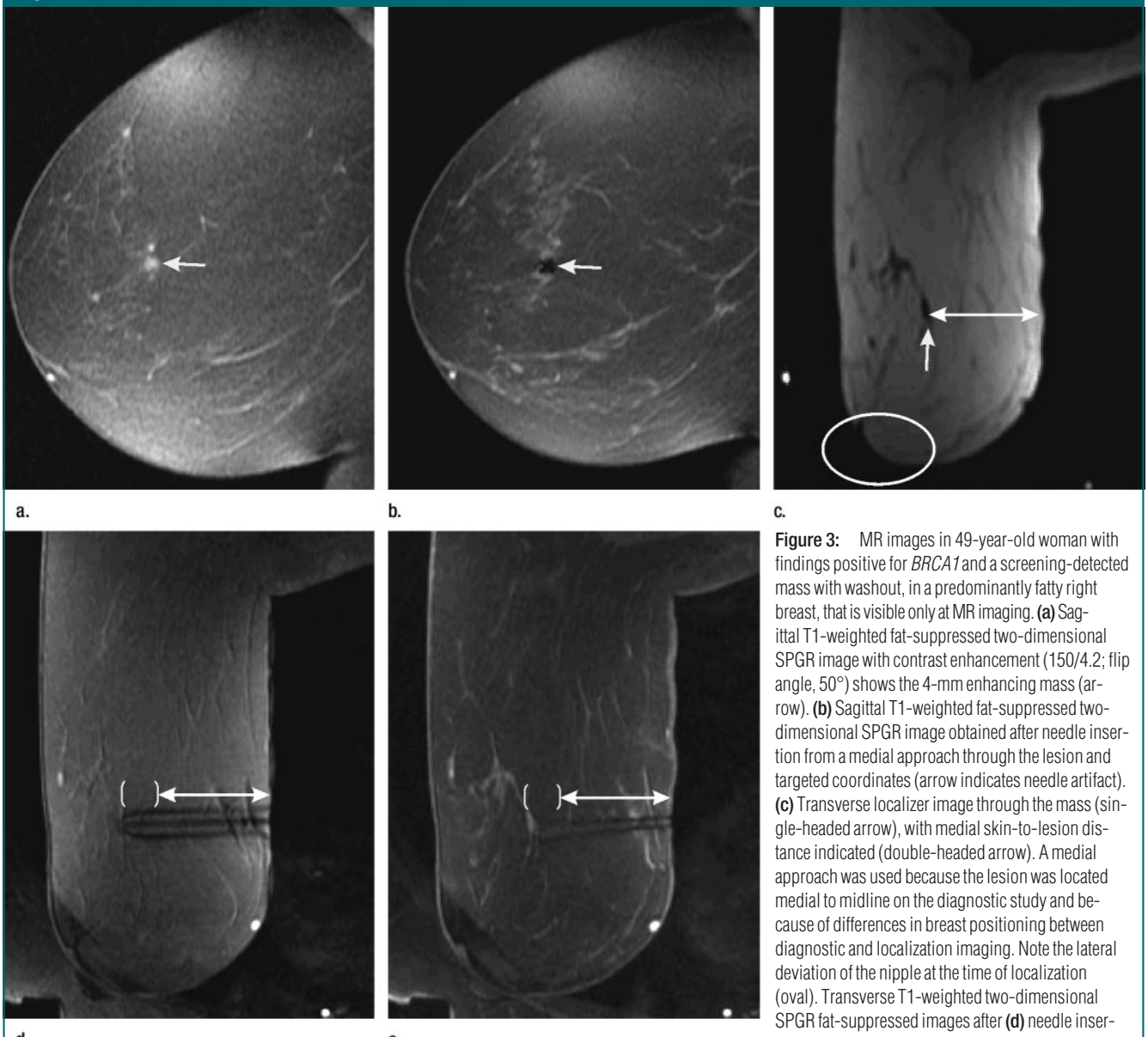

Figure 3: MR images in 49-year-old woman with findings positive for *BRCA1* and a screening-detected mass with washout, in a predominantly fatty right breast, that is visible only at MR imaging. **(a)** Sagittal T1-weighted fat-suppressed two-dimensional SPGR image with contrast enhancement (150/4.2; flip angle, 50°) shows the 4-mm enhancing mass (arrow). **(b)** Sagittal T1-weighted fat-suppressed two-dimensional SPGR image obtained after needle insertion from a medial approach through the lesion and targeted coordinates (arrow indicates needle artifact). **(c)** Transverse localizer image through the mass (single-headed arrow), with medial skin-to-lesion distance indicated (double-headed arrow). A medial approach was used because the lesion was located medial to midline on the diagnostic study and because of differences in breast positioning between diagnostic and localization imaging. Note the lateral deviation of the nipple at the time of localization (oval). Transverse T1-weighted two-dimensional SPGR fat-suppressed images after **(d)** needle insertion and **(e)** wire deployment demonstrate the degree of tissue shift in the z (depth) plane. Placement of the tip of the needle, although accurate according to prelocalization coordinates and wire artifact are just short of the lesion. Double-headed arrows indicate the skin-to-lesion distance for preinsertion MR imaging. Parentheses indicate the difference in distance from the lesion position to the original MR imaging lesion coordinates.

low-up rate of 38.4% (28). The accordion effect and subsequent backing out of the wire placed in the z direction have been a recognized explanation for missed lesions after MR-guided needle localizations (28). This explanation would be logical for each of our missed lesions, as they were located just at the deep end, adjacent to the surgical biopsy scar. The alternative possibility that our slightly higher miss rate was related to shortcomings in our system must be considered. However, the needle and wire placement technique and the actual grid compression localizing devices we used are similar to those previously reported as highly successful (28,39), making this explanation unlikely. Furthermore, the findings of MR imaging performed after wire placement document that the wire is accurately placed, therefore indicating that the final surgical miss rate is due to some postplacement factor.

We attempted to combat this unexpected occurrence by obtaining one additional set of transverse images after wire insertion, after release of the mild mediolateral compression, for the last five patients (16%) in our series. It is concerning that the additional confirmatory transverse imaging was performed for one of the missed lesions. This transverse image showed that the wire was accurately placed through and 11 mm beyond the lesion targeted. Therefore, wire movement or migration between localization and surgery is another concern, and it is also recognized in the MR imaging and mammographic literature (21,40–43). However, this particular lesion was unusually difficult to localize owing to its medial and very posterior position in the breast against the chest wall. A lateral approach was used, as this was the only access that allowed the needle to reach the lesion. The shorter medial access would have placed the needle too far anterior to the target, because of the thickness of soft tissue anterior to the sternum.

In two of 33 patients (6%), lesions were recommended for biopsy but not seen at the time of the procedure or at subsequent imaging. This rate of biopsy cancellation due to lesion resolution is similar to the 4.7% reported by Morris et al (28).

Because our system is not commercially available, the use of our study protocol is limited to our center. However, our goal was to determine the accuracy of the system being used at our institution. Our imaging protocol changed for the last five patients (16%) to include imaging in the transverse plane before and after needle and wire insertion, and this change may have introduced variability in our results. This addition, however, was designed to improve accuracy in through-plane positioning. One last limitation, as in any breast MR imaging localization study, was the inability to image the specimen directly to verify lesion retrieval.

In conclusion, our system offers a relatively quick and accurate means for performing preoperative MR-guided needle localizations in the breast. The addition of a medial access approach optimized surgical management and was used for a substantial number of patients. Factors that increase the degree of error in needle placement include small lesion size in fatty breasts and tissue shift in the transverse plane. Perpendicular plane imaging before and after needle placement is useful for identifying the degree of tissue shift, which may require adjustment of needle position.

References

1. Morris EA. Review of breast MRI: indications and limitations. Semin Roentgenol 2001;36:226–237.
2. LaTrenta LR, Menell JH, Morris EA, Abramson AF, Dershaw DD, Liberman L. Breast lesions detected with MR imaging: utility and histopathologic importance of identification with US. Radiology 2003;227:856–861.
3. Kuhl CK, Morakkabati N, Leutner CC, Schmiedel A, Wardelmann E, Schild HH. MR imaging–guided large-core (14 gauge) needle biopsy of small lesions visible at breast MR imaging alone. Radiology 2001; 220:31–39.
4. Warner E, Plewes D, Hill K, et al. Surveillance of BRCA1 and BRCA2 mutation carriers with magnetic resonance imaging, ultrasound, mammography and clinical breast examination. JAMA 2004;292(11):1317–1325.
5. Harms SE, Flamig DP, Hesley KL, et al. MR imaging of the breast with rotating delivery of excitation off resonance: clinical experience with pathologic correlation. Radiology 1993;187:493–501.
6. Orel SG, Schnall MD, LiVolsi VA, Troupin RH. Suspicious breast lesions: MR imaging with radiologic-pathologic correlation. Radiology 1994;190:485–493.
7. Kaiser WA, Zeitler E. MR imaging of the breast: fast imaging sequences with and without Gd-DTPA. Preliminary observations. Radiology 1989;170:681–686.
8. Heywang SH, Wolf A, Pruss E, Gilbertz T, Eiermann W, Permanetter W. MR imaging of the breast with Gd-DTPA: use and limitations. Radiology 1989;171:95–103.
9. Soderstrom CE, Harms SE, Copit DS, et al. Three-dimensional RODEO breast MR imaging of lesions containing ductal carcinoma in situ. Radiology 1996;201:427–432.
10. Orel SG, Mendonca MH, Reynolds C, Schnall MD, Solin LJ, Sullivan DC. MR imaging of ductal carcinoma in situ. Radiology 1997;202:413–420.
11. Gilles R, Zafrani B, Guinebretiere JM, et al. Ductal carcinoma in situ: MR imaging-histopathologic correlation. Radiology 1995; 196:415–419.
12. Ikeda DM, Birdwell RL, Daniel BL. Potential role of magnetic resonance imaging and other modalities in ductal carcinoma in situ detection. Magn Reson Imaging Clin N Am 2001;9:345–356.
13. Bone B, Pentek Z, Perbeck L, Veress B. Diagnostic accuracy of mammography and contrast-enhanced MR imaging in 238 histologically verified breast lesions. Acta Radiol 1997;38:489–496.
14. Kacl GM, Liu P, Debatin JF, Garzoli E, Caduff FR, Krestin GP. Detection of breast cancer with conventional mammography and contrast-enhanced MR imaging. Eur Radiol 1998;8:194–200.
15. Kuhl CK, Mielcareck P, Klaschik S, et al. Dynamic breast MR imaging: are signal intensity time course data useful for differential diagnosis of enhancing lesions? Radiology 1999;211:101–110.
16. Fischer U, Kopka L, Grabbe E. Breast carcinoma: effect of preoperative contrast-enhanced MR imaging on the therapeutic approach. Radiology 1999;213:881–888.
17. Bone B, Wiberg MK, Szabo BK, Szakos A, Danielsson R. Comparison of 99mTc-sestamibi scintimammography and dynamic MR imaging as adjuncts to mammography in the diagnosis of breast cancer. Acta Radiol 2003; 44:28–34.

18. Heywang-Kobrunner SH, Bick U, Bradley WG Jr, et al. International investigation of breast MRI: results of a multi-centre study (11 sites) concerning diagnostic parameters for contrast-enhanced MRI based on 519 histopathologically correlated lesions. Eur Radiol 2001;11:531–546.

19. Morris EA. Screening for breast cancer with MRI. Semin Ultrasound CT MR 2003;24:45–54.

20. Orel SG, Schnall MD, Newman RW, Powell CM, Torosian MH, Rosato EF. MR imaging-guided localization and biopsy of breast lesions: initial experience. Radiology 1994; 193:97–102.

21. Heywang-Kobrunner SH, Huynh AT, Viehweg P, Hanke W, Requardt H, Paprosch I. Prototype breast coil for MR-guided needle localization. J Comput Assist Tomogr 1994; 18:876–881.

22. Fischer U, Bosshenrich R, Gruhn H, Keating D, Raab BW, Oestmann JW. MR-guided localization of suspected breast lesions detected exclusively by postcontrast MRI. J Comput Assist Tomogr 1995;19:63–66.

23. Orel SG, Schnall MD, Powell CM, et al. Staging of suspected breast cancer: effect of MR imaging and MR-guided biopsy. Radiology 1995;196:115–122.

24. Kuhl CK, Elevelt A, Leutner CC, Gieseke J, Pakos E, Schild HH. Interventional breast MR imaging: clinical use of a stereotactic localization and biopsy device. Radiology 1997;204:667–675.

25. Daniel BL, Birdwell RL, Ikeda DM, et al. Breast lesion localization: a freehand, interactive MR imaging-guided technique. Radiology 1998;207:455–463.

26. Fischer U, Kopka L, Grabbe E. Magnetic resonance guided localization and biopsy of suspicious breast lesions. Top Magn Reson Imaging 1998;9:44–59.

27. Heywang-Kobrunner SH, Heinig A, Schaumloeffel-Schulze U, et al. MR-guided percutaneous excisional and incisional biopsy of breast lesions. Eur Radiol 1999;9:1656–1665.

28. Morris EA, Liberman L, Dershaw DD, et al. Preoperative MR imaging-guided needle localization of breast lesions. AJR Am J Roentgenol 2002;178:1211–1220.

29. Schneider JP, Schulz T, Horn LC, Leinung S, Schmidt F, Kahn T. MR-guided percutaneous core biopsy of small breast lesions: first experience with a vertically open 0.5T scanner. J Magn Reson Imaging 2002;15:374–385.

30. Viehweg P, Heinig A, Amaya B, Alberich T, Laniado M, Heywang-Kobrunner SH. MR-guided interventional breast procedures considering vacuum biopsy in particular. Eur J Radiol 2002;42:32–39.

31. Perlet C, Heinig A, Prat X, et al. Multicenter study for the evaluation of a dedicated biopsy device for MR-guided vacuum biopsy of the breast. Eur Radiol 2002;12:1463–1470.

32. Liberman L, Morris EA, Dershaw DD, Thornton CM, Van Zee KJ, Tan LK. Fast MRI-guided vacuum-assisted breast biopsy: initial experience. AJR Am J Roentgenol 2003;181:1283–1293.

33. Orel SG, Schnall MD, Mies CJ. MRI-compatible 12-G vacuum-assisted core biopsy of suspicious enhancing lesions: preliminary experience (abstr). In: Radiological Society of North America Scientific Assembly and Annual Meeting Program. Oak Brook, Ill: Radiological Society of North America, 2003; 493.

34. Warner E, Plewes DB, Shumak RS, et al. Comparison of breast magnetic resonance imaging, mammography, and ultrasound for surveillance of women at high risk for hereditary breast cancer. J Clin Oncol 2001;19: 3524–3531.

35. Konyer NB, Ramsay EA, Bronskill MJ, Plewes DB. Comparison of MR imaging breast coils. Radiology 2002;222:830–834.

36. Greenman RL, Lenkinski RE, Schnall MD. Bilateral imaging by using separate interleaved 3D volumes and dynamically switched multiple receive coil arrays. Magn Reson Med 1998;39:108–115.

37. American College of Radiology. Breast imaging reporting and data system (BI-RADS). 4th ed. Reston, Va: American College of Radiology, 2003.

38. Liberman L, Dershaw DD, Morris EA. Abramson AF, Thorton CM, Rosen PP. Clip placement after stereotactic vacuum-assisted breast biopsy. Radiology 1997;205: 417–422.

39. Schneider E, Rohling KW, Schnall MD, Giaquinto RO, Morris EA, Ballon D. An apparatus for MR-guided breast lesion localization and core biopsy: design and preliminary results. J Magn Reson Imaging 2001;14:243–253.

40. Jackman RJ, Marzoni FA. Needle-localization breast biopsy: why do we fail? Radiology 1997;204:677–684.

41. Owen AW, Kumar EN. Migration of localizing wires used in guided biopsy of the breast. Clin Radiol 1991;43:251.

42. Davis PS, Wechsler RJ, Feig SA, March DE. Migration of breast biopsy localization wire. AJR Am J Roentgenol 1988;150:787–788.

43. van Susante JL, Barendregt WB, Bruggink ED. Migration of the guide-wire into the pleural cavity after needle localization of breast lesions. Eur J Surg Oncol 1998;24: 446–448.